arXiv:1203.1860v1 [astro-ph.HE] 8 Mar 2012

The gamma-ray spectrum of Geminga and the inverse Compton model of pulsar high energy emission

Maxim Lyutikov
Department of Physics, Purdue University,
525 Northwestern Avenue, West Lafayette, IN 47907-2036

ABSTRACT

We reanalyze the Fermi spectra of the Geminga and Vela pulsars. We find that the spectrum of Geminga above the break is exceptionally well approximated by a simple power law without the exponential cut-off, making Geminga's spectrum similar to that of Crab. Vela's broadband gamma-ray spectrum is equally well fit with both the exponential cut-off and the double power law shapes.

In the broadband double power-law fits, for a typical Fermi spectrum of a bright γ-ray pulsar, most of the errors accumulate due to the arbitrary parametrization of the spectral roll-off. In addition, a power law with an exponential cut-off gives an acceptable fit for the underlying double power-law spectrum for a very broad range of parameters, making such fitting procedures insensitive to the underlying Fermi photon spectrum.

Our results have important implications for the mechanism of pulsar high energy emission. A number of observed properties of γ-ray pulsars, *i.e.*, the broken power law spectra without exponential cut-offs and stretching in case of Crab beyond the maximal curvature limit, spectral breaks close to or exceeding the maximal breaks due to curvature emission, a Crab patterns of relative intensities of the leading and trailing pulses repeated in the X-ray and γ-ray regions, all point to the inverse Compton origin of the high energy emission from majority of pulsars.

1. VERITAS detection of Crab pulsar: a case for inverse Compton scattering origin of γ-ray emission

The recent launch of the *Fermi* Gamma-Ray Space Telescope and subsequent detection of a large number of pulsars (Abdo 2010d) revolutionized our picture of the non-thermal emission from pulsars in the gamma-ray band from 100 MeV up to about 10 GeV. At even higher energies, in the very-high energy (VHE) band, the detection of the Crab pulsar at 25 GeV by the Magic Collaboration (Aliu & MAGIC Collaboration 2008) and recently at

120 GeV by the VERITAS Collaboration (VERITAS Collaboration & Aliu 2011) in the very-high energy (VHE) band allow to stringently constrain the very-high-energy emission mechanisms in the case of the Crab pulsar.

Lyutikov et al. (2011) have argued that in case of Crab the inverse Compton scattering is the main emission mechanism of the very high energy emission. This was based on the detection of Crab pulsar by VERITAS collaboration above 150 GeV (VERITAS Collaboration & Aliu 2011) with non-exponential cut-off above the spectral break. The non-exponential cut-off was later confirmed by the MAGIC collaboration (Aleksić 2011, which also preferred IC model over the curvature emission).

The curvature emission in pulsars is limited to energies below

$$\epsilon_{br} = (3\pi)^{7/4} \frac{\hbar}{(ce)^{3/4}} \eta^{3/4} \sqrt{\xi} \, \frac{B_{NS}^{3/4} R_{NS}^{9/4}}{P^{7/4}} \tag{1}$$

where R_L is the light cylinder radius, P is pulsar period of rotation, ξ is a dimensionless scaling parameter $\xi = R_c/R_L$, R_c is the radius of curvature of magnetic field lines, $B = B_{NS}(R_{NS}/R)^3$, where B_{NS} is the magnetic field on the surface of the neutrons star and R_{NS} the stars surface and $\eta = E/B \leq 1$ is the relative strength of the accelerating electric field , (Lyutikov et al. 2011).

If the γ-ray photons are due to the curvature emission of a radiation reaction-limited population of leptons, the spectrum above the break must show an exponential cut-off. The detection of the Crab pulsar by VERITAS collaboration (VERITAS Collaboration & Aliu 2011) clearly demonstrated the non-exponential cut-off above the spectral break, see Fig. 1. Lyutikov et al. (2011) have argued that this is inconsistent with the curvature emission.

2. Spectral breaks in γ-ray pulsars

The curvature and the IC model of the high energy emission offer different interpretations of the spectral breaks. In case of the curvature emission, the spectral break corresponds to the maximal energy of the radiation reaction-limited acceleration. Above the break the spectrum is expected to have an exponential cut-off. In the IC model the spectral break corresponds to the break in particle distribution function, which is likely to be of the power law type both below and above the break. Thus, observations of the non-exponential cut-off above the break favor the IC model.

Crab pulsar is a bright emitter in all spectral bands. Thus, there is a lot of low frequency target photons available for Compton scattering. What about other pulsars? In the present

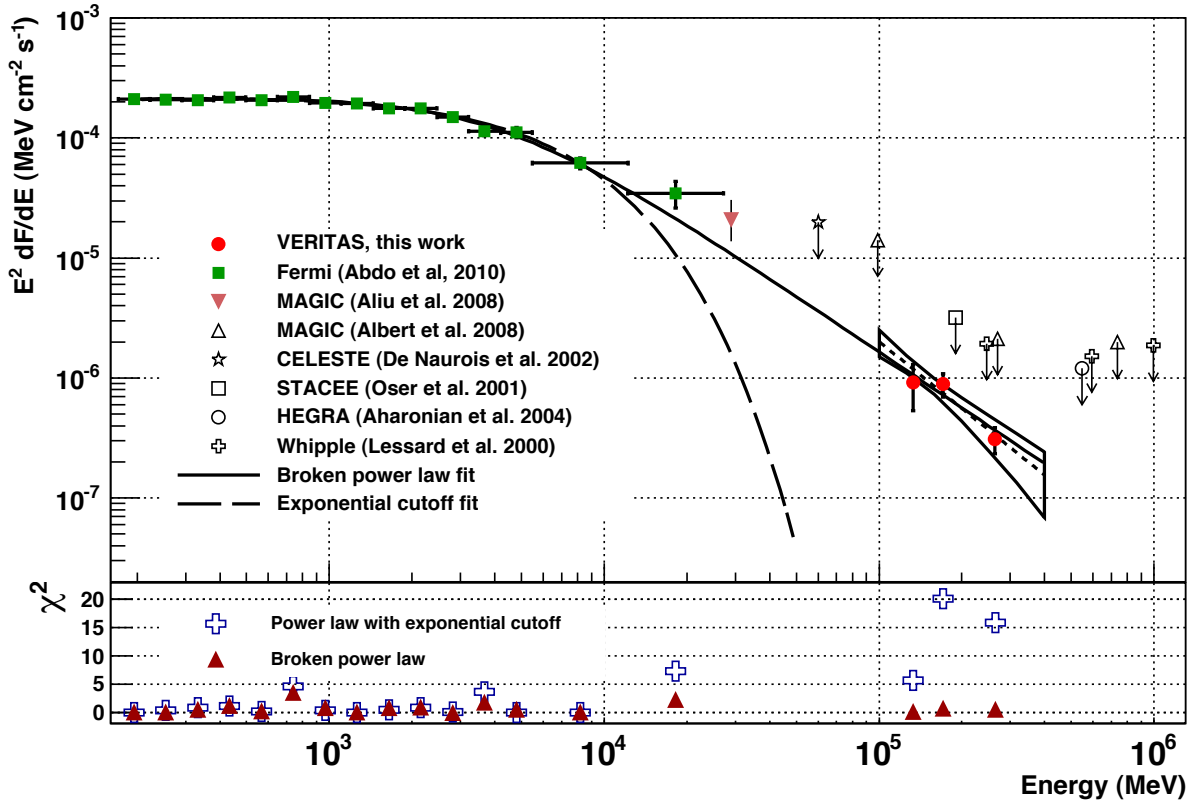

Fig. 1.— High energy spectrum of Crab demonstrating the non-exponential spectral break inconsistent with curvature emission (figure from VERITAS Collaboration & Aliu 2011) .

paper we argue that that there are evidence for a universal dominance of the inverse Compton scattering mechanism in γ-ray pulsars.

First, Lyutikov et al. (2011) compared the observed spectral breaks of Fermi pulsars from the first Fermi catalogue (Abdo 2010d) with the predicted breaks due to curvature emission, Eq. (1) by calculating the ratio of the observed E_{br} and predicted spectral break ϵ_{br}, see Fig. 2. A significant number of pulsars the ratio is close to one and for one pulsar, PSR J1836 + 5925, the ratio is even larger than one. In order to explain the spectral break for these pulsars as a result of curvature radiation, an accelerating electric fields should be close to or even larger than the magnetic fields .

What is more, the example of Crab demonstrates that the spectral break may not be related to the maximal curvature photons. The presence of non-exponential breaks in pulsars others than Crab would be a clear indication that the break is not related to maximal energy

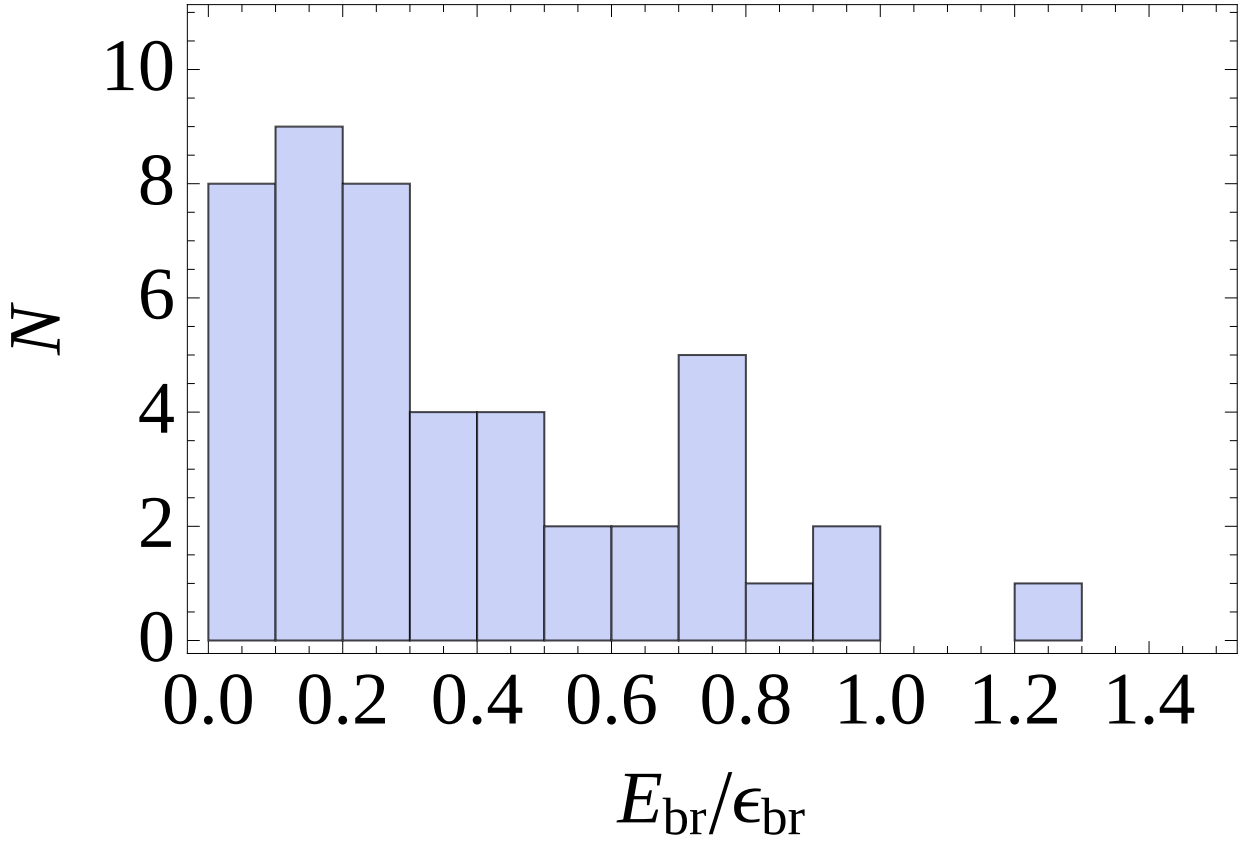

Fig. 2.— Ratio of the observed break energies E_{br} for 46 pulsars to the maximum predicted for curvature radiation ϵ_{br}, which is given by Eq. (1) with $\eta = \xi = 1$ (Lyutikov et al. 2011).

of curvature emission by radiation-limited acceleration of leptons. Realistically, due to low photon counts, only the brightest γ-ray pulsars - Crab, Vela and Geminga - allow precise enough measurements of fluxes to distinguish between different spectral shapes. In addition, typically, only phased average properties have enough photon counts to distinguish between the models.

3. Spectra of Geminga and Vela pulsars

3.1. Geminga: a non-exponential cut-off

Geminga is one of the brightest γ-ray pulsars. Its spectrum is, conventionally, fit with a power-law plus exponential cut-off (Abdo 2010a). We have performed an independent fit to Geminga spectrum, see Table 2 and Figs. 3-4-5. For the fits, the processed data (energy

flux) provided by the Fermi collaboration were used, Table 3.1.

First, we performed χ^2 fits of the whole spectrum using a particular type of double power-law prescription (with 4 independent parameters, row (a) in Table 2, the power-law plus exponential cut-off (with 3 independent parameters, row (b) in Table 2) and a softened exponential cut-off (with 4 independent parameters, row (c) in Table 2), see Table 2 and Fig. 3. Weighted and unweighted reduced χ^2 fits were not statistically distinguishable. (Overall normalization is the additional fit parameter to the ones listed in Table 2.)

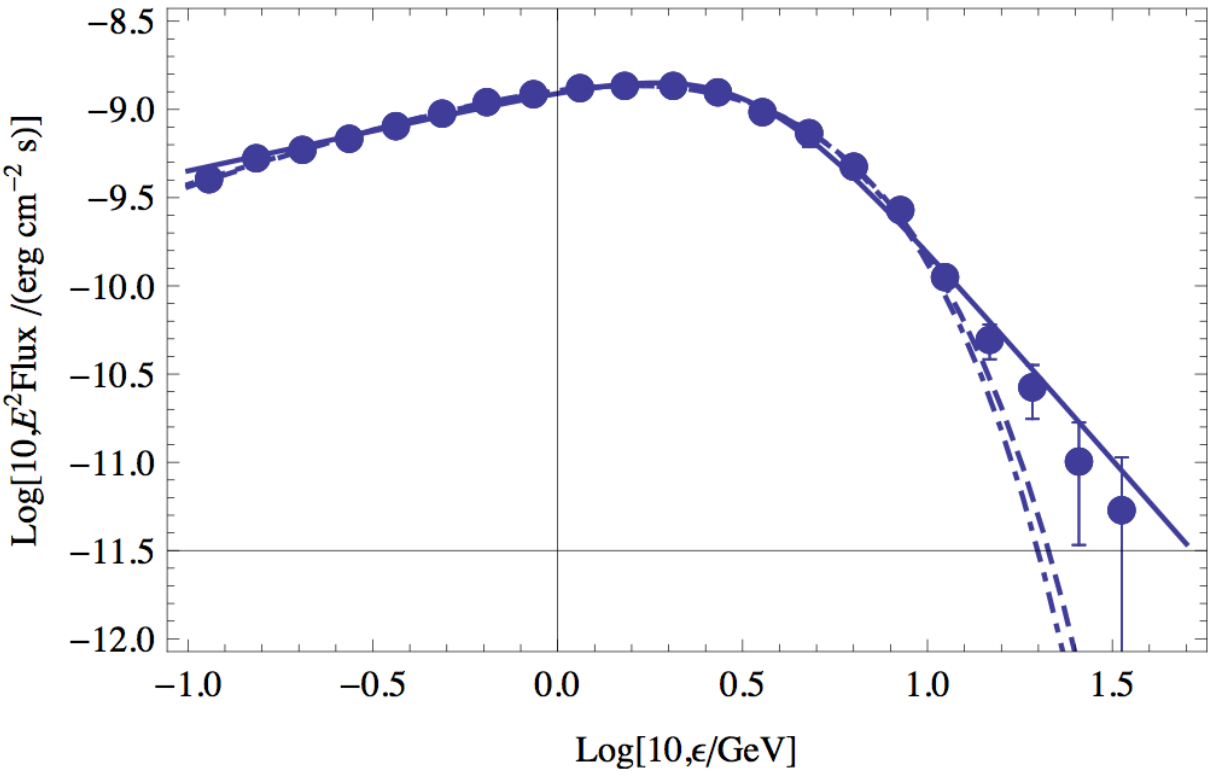

Fig. 3.— Fits to Geminga spectrum by models described in Table 2. Solid line is double power-law model (a) from Table 2 (reduced $\chi^2 = 1.26$), dot dashed is an exponential cut-off (reduced $\chi^2 = 1.13$) and dashed is a softened exponential cut-off (reduced $\chi^2 = 0.83$). Since in all cases χ^2 is of the order of unity, all three models are statistically acceptable. (See also Fig. 4 for the error analysis of the double power-law fit.)

Inspection of Table 2 and Figs. 3-4 tells, first, that since the reduced χ^2 is close to

E(GeV)	E^2 Flux ($erg\,cm^{-2}s^{-1}$)	dE^2 Flux ($erg\,cm^{-2}s^{-1}$)
0.114	4.02E-10	2.3E-11
0.153	5.29E-10	4.0E-11
0.204	5.90E-10	2.2E-11
0.273	6.82E-10	6.5E-11
0.365	8.04E-10	6.1E-11
0.487	9.47E-10	7.2E-11
0.643	1.10E-09	1.0E-10
0.860	1.22E-09	9.2E-11
1.149	1.32E-09	1.3E-10
1.518	1.36E-09	1.3E-10
2.053	1.36E-09	1.0E-10
2.711	1.25E-09	9.4E-11
3.580	9.65E-10	1.1E-10
4.785	7.34E-10	1.2E-10
6.319	4.74E-10	5.5E-11
8.446	2.69E-10	3.1E-11
11.153	1.12E-10	1.5E-11
14.728	4.94E-11	1.1E-11
19.214	2.66E-11	9.0E-12
25.681	1.01E-11	6.7E-12
33.505	5.35E-12	5.3E-12

Table 1: Phase-averaged data for Geminga pulsar.

model	Fit function	α	β	ϵ_{br}	reduced, unweighted χ^2	b	dof
a	$\left(\left(\frac{\epsilon}{\epsilon_{br}}\right)^{\alpha}+\left(\frac{\epsilon}{\epsilon_{br}}\right)^{-\beta}\right)^{-1}$	2.38	0.45	3.32	1.26	–	17
b	$\epsilon^{\beta}e^{-\frac{\epsilon}{\epsilon_{br}}}$	–	.70	2.35	1.13	–	18
c	$\epsilon^{\beta}e^{-\left(\frac{\epsilon}{\epsilon_{br}}\right)^{b}}$	–	0.75	1.98	0.83	0.91	17

Table 2: Fits to the broad band spectrum of Geminga. The values for fit (c) can be compared with the best fit done by Fermi team, $\beta = 1.12$, $\epsilon_{br} = 1.58$, $b = 0.81$, (Abdo 2010a).

unity all three models are statistically acceptable. (In Appendix 5 we also demonstrate that for a typical Fermi spectrum of a bright γ-ray pulsar a fit with an exponential cut-off can actually give a satisfactory approximation to the underlying power-law spectrum for a very wide regime of fit parameters, *e.g.,* over two orders of magnitude in break energy.)

Second, the fit that looks the best down to low flux levels, fit (a), actually has largest reduced χ^2 among the models. The errors for the this fit are accumulated at intermediate energies due to *an arbitrarily chosen parametrization of the spectral roll-off.* Since we are mostly interested in the high energy scaling of the spectrum, we can take only the highest energy points. Having chosen the last 6 points we derive the fit given in Table 3, see also Fig. 5.

Fit function	α	reduced χ^2	dof
ϵ^{α}	3.04	0.1	4

Table 3: Properties of the fit of the high energy tail of Geminga.

Thus, the high energy part of the Geminga spectrum is exceptionally well fit with a power-law function, giving reduced $\chi^2 = 0.1$. This exceptional small value of χ^2 is a bit surprising: despite the lower overall count *the highest energy data points have the smallest error bars*, Table 3.1, due to the very low background counts above ~ 2 GeVs. A small value of χ^2 for the high energy fit may be due to the fact that the fit has only four degrees of freedom - in this case the random chance for all the points being very close to the model is not small. This may also be an indication that the number of energy channels was chosen not in an optimal way, *e.g.,* too broad energy bins. (If only 5 highest energy points are used, the fit values are $\alpha = 2.8$, $\chi^2 = 0.03$ for 3 degrees of freedom.)

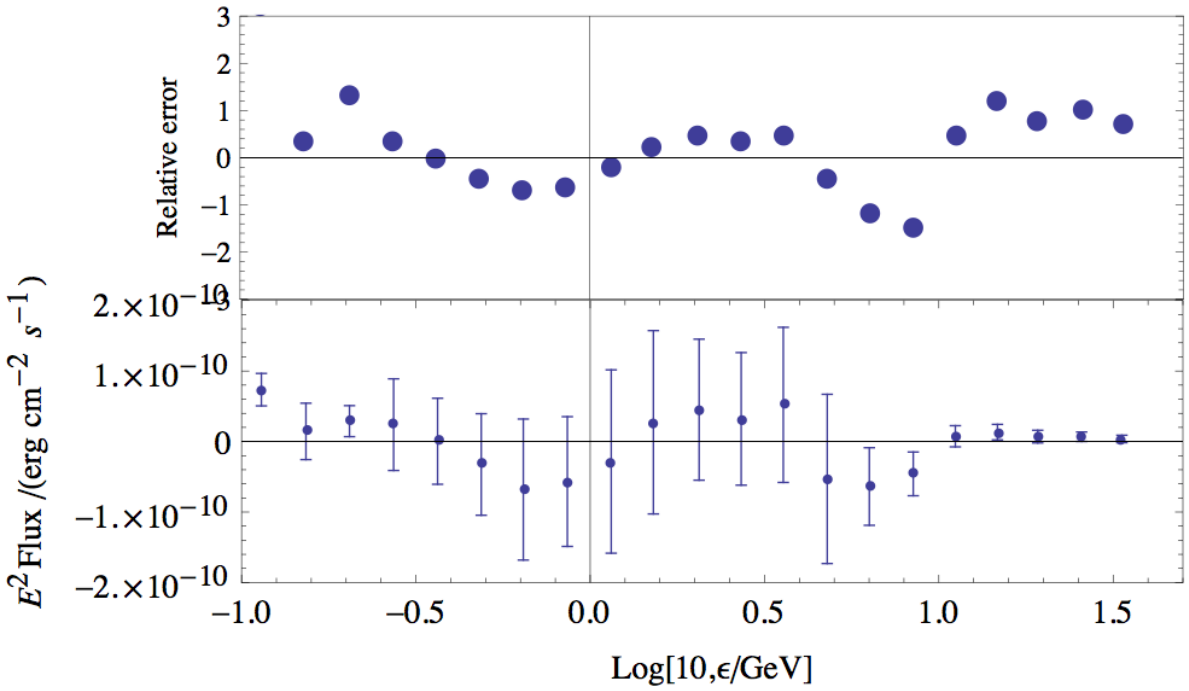

Fig. 4.— Errors for the broadband fit to Geminga data using double power law function. The lower panel shows the residuals (on a linear scale) for the double power-law fit, while the upper panel shows relative errors that are used to calculate χ^2. The errors are not random indicating the inadequacy of the arbitrarily chosen spectral roll-off. Also, most of the χ^2 is accumulated near the break energy due to the arbitrary parametrization of the spectral roll-off. Note that the highest energy data points actually have the smallest error bars.

3.1.1. Geminga to be seen at very high gamma-ray energies?

The spectral index above the break $dN/dE \propto E^{-p}$ with $p \approx 5$ for Geminga is steeper than that of the Crab pulsar ($p = 3.8$ above the break McCann & VERITAS Collaboration 2011). Geminga is nearly two and a half times brighter than Crab at the peak of its spectral distribution of $\sim 1GeV$, but its has lower break energy and most importantly the steeper spectrum. The expected flux at $\sim$ 120 GeV, the low energy threshold for the VERITAS Cherenkov telescope, is then few $\sim 10^{-8}$ MeV cm^{-2}, s^{-1}. This is approximately ten times

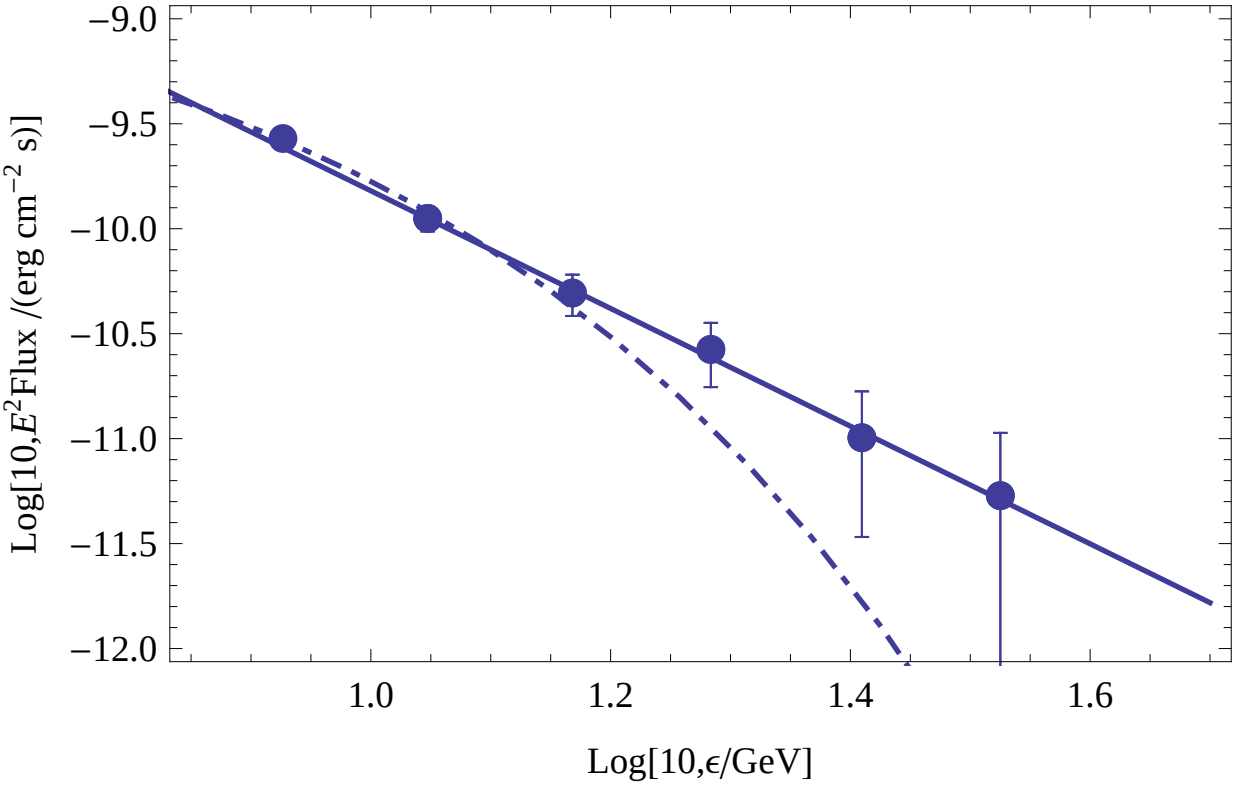

Fig. 5.— Fits to the high energy tail of the Geminga spectrum: power law (solid line, $\chi^2 = 0.1$) and exponential cut-off (dashed line, $\chi^2 = 2$).

lower than the flux from the Crab pulsar. Geminga, still, has a chance to be detected, since unlike Crab it has no strong background from the PWN. (It is not clear whether the excess TeV flux from the general direction of Geminga (Abdo et al. 2008) is related to the pulsar (see, though Salvati & Sacco 2008)).

3.1.2. Geminga: Phase-resolved fit

Phase variation in the cut-off energy can affect the overall spectral fit, *but not at the highest energies*. For example, Abdo (2010a) cite the cut-off energy variations between approximately 1 and 3 GeV, while our high energy fit starts at 8.5 GeV, nearly three times higher, see Table 3 and Fig. 5. In addition, due to a low photon count in the phase-resolved SEDs, they naturally miss the highest energy, lowest counts tails.

To test the spectral shape in phased-resolved spectra we have performed spectral fitting at one particular phase, $0.614 < \phi < 0.623$, corresponding, approximately to the second

peak Abdo (2010a). Since phase resolved data were not available, we assumed the error on the flux to be equal to 2×10^{-12}erg cm^{-2} s^{-1}, see Table 4 and Fig. 6.

model	Fit function	α	β	ϵ_{br}	reduced, unweighted χ^2	b	dof
a	$\left(\left(\frac{\epsilon}{\epsilon_{br}}\right)^{\alpha} + \left(\frac{\epsilon}{\epsilon_{br}}\right)^{-\beta}\right)^{-1}$	2.08	0.69	3.61	0.46	–	6
b	$\epsilon^{\beta} e^{-\frac{\epsilon}{\epsilon_{br}}}$	–	0.97	2.43	0.23	–	7

Table 4: Parameters for the phase-resolved fit of Geminga.

Thus, both the double power-law and the exponential cut-off provide a statistically viable description of data for a particular phase-resolved spectrum of Geminga.

3.2. Vela: consistent with the non-exponential tail

Vela, the brightest γ-ray pulsar, offers tantalizing, but non-conclusive evidence of the non-exponential break, see Fig. 7. We performed an unweighted χ^2 fit with phase-averaged data provided by the Fermi collaboration, Table 3.2. We used various double power-law prescriptions (with 4 independent parameters), the power-law plus exponential cut-off (with 3 independent parameters) and a softened exponential cut-off (with 4 independent parameters), see Table 6. Spectrum of Vela is equally well fit with a softened exponential cut-off and a double power-law spectrum.

In case of Vela, a particular choice of the parametrization of the double power-law spectrum illustrates that an arbitrary choice of the roll-off between the two spectral power-law components has an important effect on the fit: while the more conventional double power-law parametrization in line (a), Table 6, gives unacceptable fit, double power-law spectrum parametrization in line (b) in Table 6 gives an acceptable fit.

4. Optical-X-ray-γ-ray correlation

Within the framework of the SSC model the power emitted by IC is related to the power of the seed photons. Photons of different energies that are emitted by the same particles should in principle produce similar pulse profiles. In our model one expects, therefore, that the pulse profiles in X-ray and in gamma-rays are similar because the secondary plasma emits synchrotron radiation in X-rays and IC scatters UV photons into the VHE band. And indeed, the ratio of the amplitudes of the two pulses in the pulse profile of the Crab pulsar

E (GeV)	E^2dN/dE ($GeV\,cm^{-2}\,s^{-1}$)	Δ E^2 dN/dE ($GeV\,cm^{-2}\,s^{-1}$)
1.117101E-01	1.162739E-09	3.340227E-11
1.406211E-01	1.498706E-09	2.520782E-11
1.770114E-01	1.595459E-09	2.106914E-11
2.228146E-01	1.686333E-09	1.978347E-11
2.804637E-01	1.884574E-09	1.960196E-11
3.530192E-01	2.056793E-09	2.013993E-11
4.443313E-01	2.195488E-09	2.126256E-11
5.592426E-01	2.313047E-09	2.269755E-11
7.038429E-01	2.432161E-09	2.455590E-11
8.857895E-01	2.559430E-09	2.698647E-11
1.114708E+00	2.605548E-09	2.954981E-11
1.402695E+00	2.601159E-09	3.249238E-11
1.764951E+00	2.555662E-09	3.546979E-11
2.220567E+00	2.399446E-09	3.841962E-11
2.793512E+00	2.103038E-09	4.017982E-11
3.513868E+00	1.772092E-09	4.120424E-11
4.419371E+00	1.587057E-09	4.349206E-11
5.557327E+00	1.228406E-09	4.282005E-11
6.987010E+00	8.144106E-10	3.878978E-11
8.782625E+00	5.932086E-10	3.699830E-11
1.103701E+01	3.489809E-10	3.221406E-11
1.386622E+01	2.072424E-10	2.828281E-11
1.741518E+01	9.641950E-11	2.123657E-11
2.186479E+01	7.252995E-11	2.044876E-11
2.744061E+01	6.922606E-11	2.403077E-11

Table 5: Phase-averaged data for Vela pulsar.

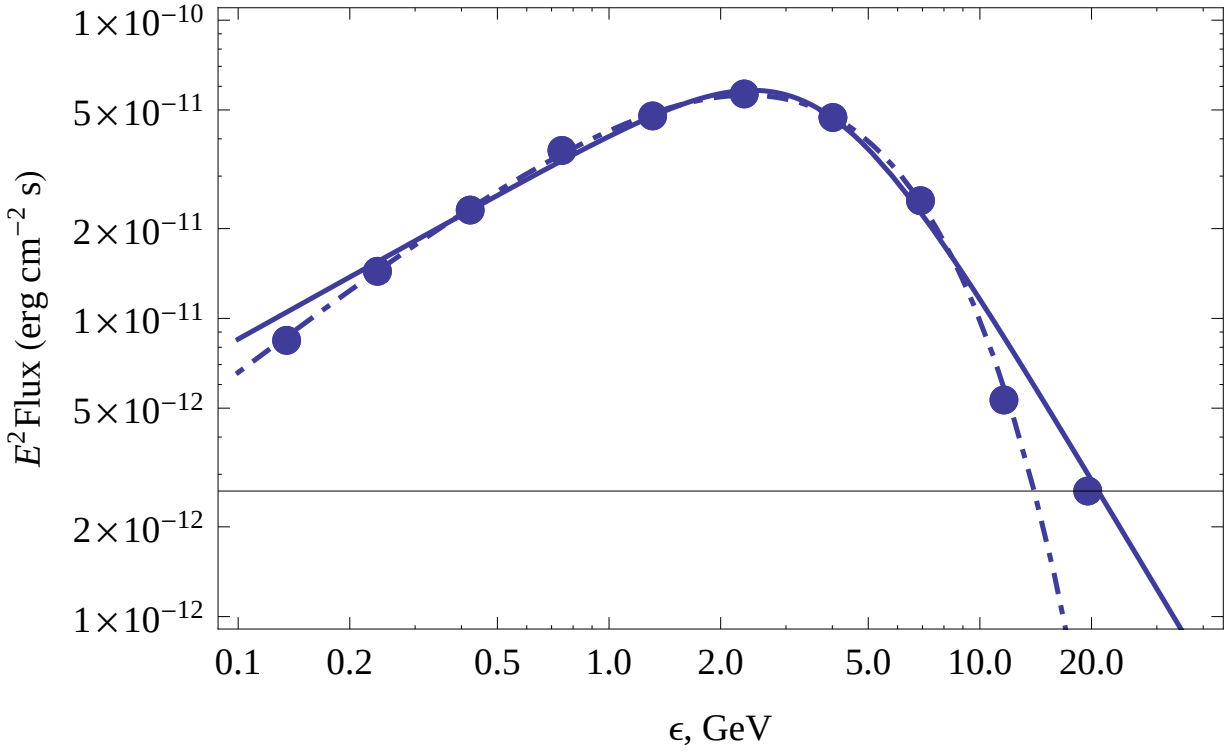

Fig. 6.— Phase-resolved fit to Geminga spectrum using double power law (solid line, reduced $\chi^2 = 0.46$) and exponential cut-off (dot dashed line, reduced $\chi^2 = 0.23$). The fit corresponds to the phase $0.614 < \phi < 0.623$ of Abdo (2010a).

model	Fit function	α	β	ϵ_{br}	reduced χ^2	b	dof
a	$\left(\left(\frac{\epsilon}{\epsilon_{br}}\right)^{\alpha} + \left(\frac{\epsilon}{\epsilon_{br}}\right)^{-\beta}\right)^{-1}$	1.68	0.34	2.91	2.2	–	21
b	$\left(\left(\frac{\epsilon}{\epsilon_{br}}\right) + \left(\frac{\epsilon}{\epsilon_{br}}\right)^{-\beta}\right)^{-\alpha}$	4.11	0.11	8.8	1.3	–	21
c	$\epsilon^{\beta} e^{-\frac{\epsilon}{\epsilon_{br}}}$	–	.42	3.1	2.0	–	22
d	$\epsilon^{\beta} e^{-\left(\frac{\epsilon}{\epsilon_{br}}\right)^{b}}$	–	0.59	1.58	1.4	0.73	21

Table 6: Parameters of the spectral fit for Vela pulsar

changes consistently in the X-rays / soft gamma-ray band and in the high energy gamma-ray band, see Fig. 8. In X-rays the main pulse dominates over the inter pulse. The ratio changes towards higher energies and reverses in the soft gamma-ray band at about 1 MeV. Mirroring the evolution at lower energy, the main pulse dominates at 100 MeV, while at

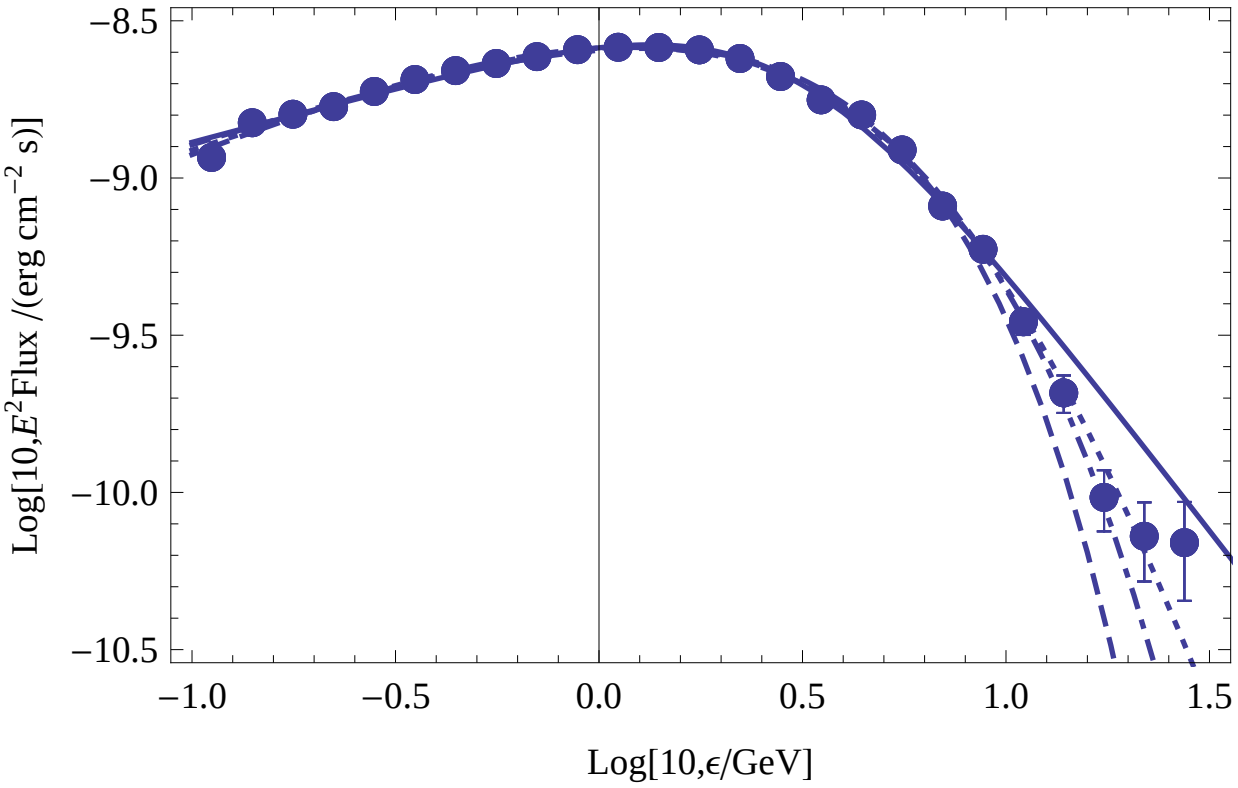

Fig. 7.— Fits to Vela spectrum by models described in Table 6. Solid line: model (a), dotted line: model (b), dashed line: model (c), dot dashed line: model (d) from Table 6. Models (a) and (b) are double power-laws, (c) is an exponential cut-off and (d) is a softened exponential cut-off. Models (a) and (c), as well as models (b) and (d) have approximately the same reduced χ^2.

120 GeV the interpulse clearly again dominates over the main pulse (Abdo 2010d; VERITAS Collaboration & Aliu 2011).

Vela also offers tantalizing evidence for the correlation between the optical/X-ray and γ-ray bands, Fig. 9: all three γ-ray peaks (P1, P2 and P3 in the top panel) have lower frequency analogues: P1 in the X-rays, P2 in optical and P3 in both bands. This is expected in the IC model, though relative intensities and spectra of the components depend on the details of the photon and particle distribution.

Crab pulsar is somewhat exceptional among the brightest X-ray-γ-ray pulsars since it has no indication of the thermal component. The X-ray emission of Vela and Geminga are strongly dominated by the thermal components coming form the surface (Halpern & Ruderman 1993; Pavlov et al. 2001; Manzali et al. 2007). In Vela, the non-thermal component

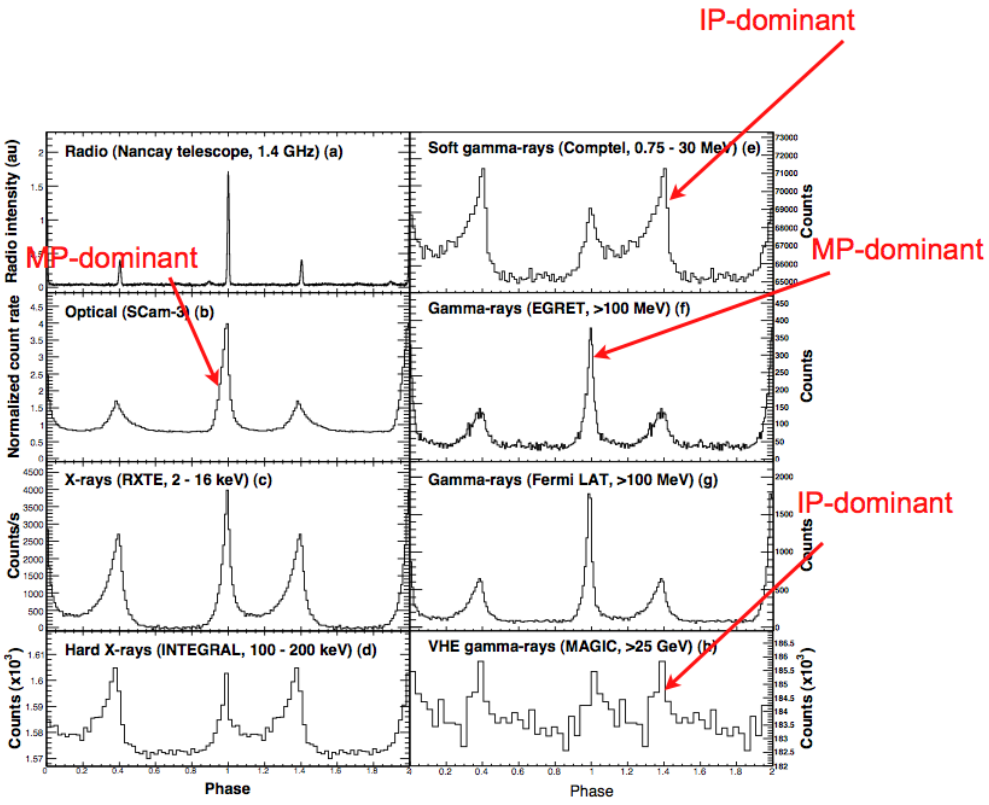

Fig. 8.— Evolution of the Crab profile with energy (Abdo 2010c). Note that that the lower-energy evolution of the increasing interpulse to main pulse ratio is mirrored in the γ-rays. Such behavior is expected in synchrotron-self-Compton model (Lyutikov et al. 2011).

in X-rays is barely detected at some orbital phases, roughly aligned with the γ-ray peaks, especially with P2, see Fig. 9 of Manzali et al. (2007). The relative weakness of the non-thermal X-ray components does not allow a measurement of the evolution of the P1/P2 ratio with energy, like in Crab. Overall, both Vela and Geminga spectra show a complicated phase- and energy-dependent mix of thermal and non-thermal components (*e.g.,* Kargaltsev et al. 2005; Romani et al. 2005). In both cases the optical emission, the main target for IC scattering, is highly non-thermal.

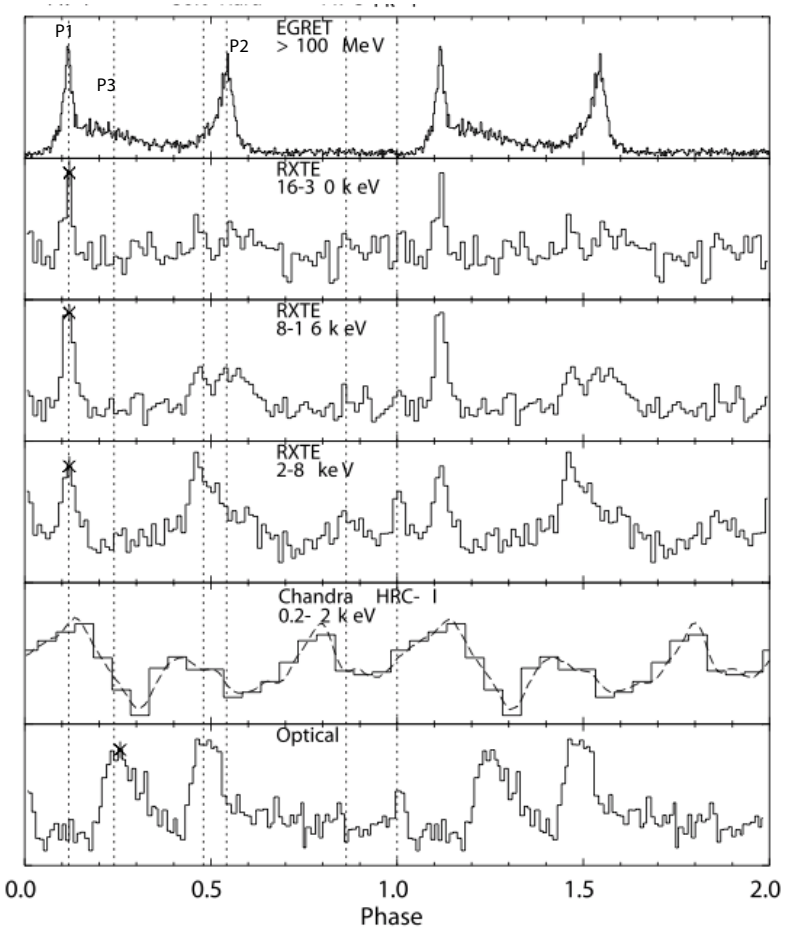

Fig. 9.— Vela profile in broad energy bands (Abdo 2010b). Chandra profile in the soft X-rays is dominated by thermal emission and is not of interest here. Optical and RXTE signals are mostly non-thermal. Note that all three γ-ray peaks (P1, P2 and P3 in the top panel) have lower frequency non-thermal analogues: P1 in the X-rays, P3 in optical and P2 in both bands. This is expected in the IC model, though the spectra and relative intensities depend on the details of the photon and particle spectra.

5. Discussion

In this paper we demonstrate that, first, broadband pulsar high energy spectra are generally consistent with the double power law shapes. This results is based on three brightest γ-ray pulsars. In Geminga the high energy part of the SED is exceptionally well fit with a power law, while the spectrum of Vela is inconclusive. Importantly, in Geminga most errors in the broadband double power law fit are accumulated due to an *arbitrary parametrization of the spectral roll-off between the two asymptotic power laws*. Thus, the standard χ^2 fit

underestimates the goodness of fit in this particular case. In addition, the low background at high energies, above 2 GeV, make Fermi data especially sensitive (smallest error bars) to the shape of the high energy spectrum.

If pulsar spectra generally show non-exponential cut-offs, a fact well established in the Crab pulsar by VERITAS (VERITAS Collaboration & Aliu 2011) and in Geminga in the present paper, this has important implications for models of pulsar γ-ray emission. This implies the importance of the inverse Compton (IC) scattering for the production of γ-ray photons (Lyutikov et al. 2011) and would signify a paradigm shift in the study of pulsar high-energy emission.

Lyutikov et al. (2011) argued that in Crab and in a number of other pulsars the inverse Compton scattering is the main emission mechanism of the very high energy emission. The authors tried to give the most general arguments in favor of IC, mostly independent of the numerous possible particular details of a full radiative model. Overall, Lyutikov et al. (2011) adopted the Cheng et al. (1986) paradigm of pulsar high energy emission, but with inverse Compton scattering playing a more important role that previously assumed. Recall, that Cheng et al. (1986) argued that IC scattering is not dominant in Crab, but may be important for Vela. VERITAS and MAGIC results on Crab indicate that IC is the dominant mechanism in Crab.

In the model of Lyutikov et al. (2011) the inverse Compton scattering occurring in the Klein-Nishina regime by the secondary particles results in a picture that, overall, is consistent with observations without any fine-tuning. The key features of our model are (i) A population of primaries that is accelerated in a modest electric field, which is a fraction η of the magnetic field strength near the light cylinder with a typical value of η is 10^{-2}. The suppression of the scattering cross-section in the Klein-Nishina regime (and the corresponding lower radiation loss rate of electrons) allows primary leptons to be accelerated to very high energies with hard spectra. (ii) The gain in energy of the primaries in the electric field is balanced by similar curvature radiation and IC losses (radiation reaction limited); (iii) The secondary plasma is less energetic, but more dense and has approximately the same energy content as the primary beam. The secondary plasma is responsible for the soft UV-X-ray emission via synchrotron/cyclotron emission and the high energy γ-ray emission that extends to hundreds of GeV via the inverse Compton process. The IC emission from the primary beam extends well into the TeV regime but will be difficult to detected due to the low predicted fluxes.

The spectra of all three brightest γ-ray pulsars are consistent with the broken power-law distribution (and, thus, with the inverse Compton origin of the γ-ray emission). What is more, Crab and Geminga are inconsistent with exponential cut-off (and, thus, with the curvature origin of the γ-ray emission). Thus, inverse Compton scattering may be the

dominant radiation mechanism in all pulsars, though a curvature contribution in some pulsars cannot be excluded.

In the analysis we use the processed data points provided by the Fermi collaboration as well as data from the published papers. These data points are actually somewhat dependent on the model used to derive them, since the model of the spectrum goes into untangling the data from the instrument response. This introduces some uncertainty, but since we are looking at the brightest pulsars we expect that a particular model used to estimate the flux in individual spectral bins is not going to make too much of a difference. We would like to encourage the community to test our results using the raw count rates data.

It is not clear what parameters determine the dominance of the IC scattering among Vela, Crab and Geminga. Calculations of Cheng et al. (1986) suggested that IC scattering may be important for Vela, but our results suggest that Vela is the weakest case for the IC among the three. The case for dominance of IC scattering in Crab was, partially, expected due to high soft photon luminosity (*e.g.,* Hirotani 2007). What is more, the Crab emission is completely non-thermal and originates in the same region of the magnetosphere as the γ-ray emission, while in Vela and Geminga a large contribution to X-ray emission comes from the thermal emission from the surface.

In addition, the strong energy dependence of IC scattering in the KN regime favors the lower energy optical-UV photons. In this view, the example of non-exponential cut-off in Geminga, and the implied importance of the IC scattering, are quite surprising given the low observed optical-X-ray luminosity. This poses challenges for radiative modeling. It is likely to be related to the fact that inverse Compton scattering is highly dependent on the details of both the soft photon distribution and the particle's distribution (*e.g.,* their anisotropy).

Finally, let us recapitulate the main arguments in favor of inverse Compton scattering being the dominant pulsar radiation mechanism at GeV energies:

- The spectrum of Crab pulsar extends beyond the upper limit for curvature emission
- The beak energy in many pulsars approaches and even exceeds the upper limit for curvature emission
- In the three brightest pulsars, Crab, Geminga and possibly Vela the spectrum above the break is not exponentially suppressed, implying that the break is not due to curvature remission of leptons in the radiation reaction-limited regime
- In Crab, the energy dependence of the relative intensity of emission peaks at γ-ray energies mirrors the lower energy energy dependence, as expected in the Inverse Compton model.

I would like to thank Oleg Kargaltsev, Matthew Lister, Rafael Lang, George Pavlov, Scott Ransom and Mallory Roberts for help with the data analysis, Roger Blandford, John Finley, Andrew McCann, Roger Romani, Nepomuk Otte, Mark Thieling and David Thompson for comments on the manuscript and Fermi Large Area Telescope Collaboration for providing Vela & Geminga phase-averaged data.

REFERENCES

Abdo, A. A. *et al.* . 2010a, ApJ, 720, 272

—. 2010b, ApJ, 713, 154

Abdo, A. A., Allen, B., Aune, T., Berley, D., Blaufuss, E., Casanova, S., Chen, C., Dingus, B. L., Ellsworth, R. W., Fleysher, L., Fleysher, R., Gonzalez, M. M., Goodman, J. A., Hoffman, C. M., Hüntemeyer, P. H., Kolterman, B. E., Lansdell, C. P., Linnemann, J. T., McEnery, J. E., Mincer, A. I., Nemethy, P., Noyes, D., Pretz, J., Ryan, J. M., Parkinson, P. M. S., Shoup, A., Sinnis, G., Smith, A. J., Sullivan, G. W., Vasileiou, V., Walker, G. P., Williams, D. A., & Yodh, G. B. 2008, Physical Review Letters, 101, 221101

Abdo, A. A. *et al.*. 2010c, ApJ, 708, 1254

—. 2010d, ApJS, 187, 460

Aleksić, J. e. 2011, ApJ, 742, 43

Aliu, E. *et al.*. & MAGIC Collaboration. 2008, Science, 322, 1221

Cheng, K. S., Ho, C., & Ruderman, M. 1986, ApJ, 300, 522

Halpern, J. P. & Ruderman, M. 1993, ApJ, 415, 286

Hirotani, K. 2007, ApJ, 662, 1173

Kargaltsev, O. Y., Pavlov, G. G., Zavlin, V. E., & Romani, R. W. 2005, ApJ, 625, 307

Lyutikov, M., Otte, N., & McCann, A. 2011, ArXiv e-prints

Manzali, A., De Luca, A., & Caraveo, P. A. 2007, ApJ, 669, 570

McCann, A. & VERITAS Collaboration. 2011, ArXiv e-prints

Pavlov, G. G., Zavlin, V. E., Sanwal, D., Burwitz, V., & Garmire, G. P. 2001, ApJ, 552, L129

Romani, R. W., Kargaltsev, O., & Pavlov, G. G. 2005, ApJ, 627, 383

Salvati, M. & Sacco, B. 2008, A&A, 485, 527

VERITAS Collaboration & Aliu, E. e. 2011, Science, 334, 69

A. On the exponential fit to Fermi-like data with power-law distribution

Often, Fermi pulsar data are fit with a softened exponential function, $\propto \epsilon^{\alpha} e^{-(\epsilon/\epsilon_{br})^b}$, which is supposed to imitate variations in the exponential cut-off energy. In this appendix we address a question: if the data come from double power-law distribution, how well will they be represented by the softened exponential fit? As an example, we fit a function $f = 2/(x + 1/x)$ sampled at equally spaced logarithmic intervals from 0.1 to 40 with a typical error of 0.01 and random scatter 0.01. This choice of the parameters simulates a typical bright pulsar spectrum sampled in unites of GeV and maximum flux of the order of ~ 100 of the statistical error.

We find that the fit function provides an acceptable fit (reduced $\chi^2 \leq 1$) for an exceptionally wide range of the break energies $0.01 \leq \epsilon_{br} \leq 2$, see Fig. 10. For less bright pulsars, where due to low photon statistics the spectrum can be measured up to a lower maximal energy, the reduced χ^2 remains smaller than unity even for larger values of the fitted ϵ_{br}.

Thus, if a typical spectrum of a bright Fermi pulsar is a broken power-law, the spectral fit with a softened exponential function, $\propto \epsilon^{\alpha} e^{-(\epsilon/\epsilon_{br})^b}$, gives acceptable fits for a very wide range of parameters and, thus, does not provide a sufficiently sensitive probe of the underlying spectrum.

This preprint was prepared with the AAS LaTeX macros v5.2.

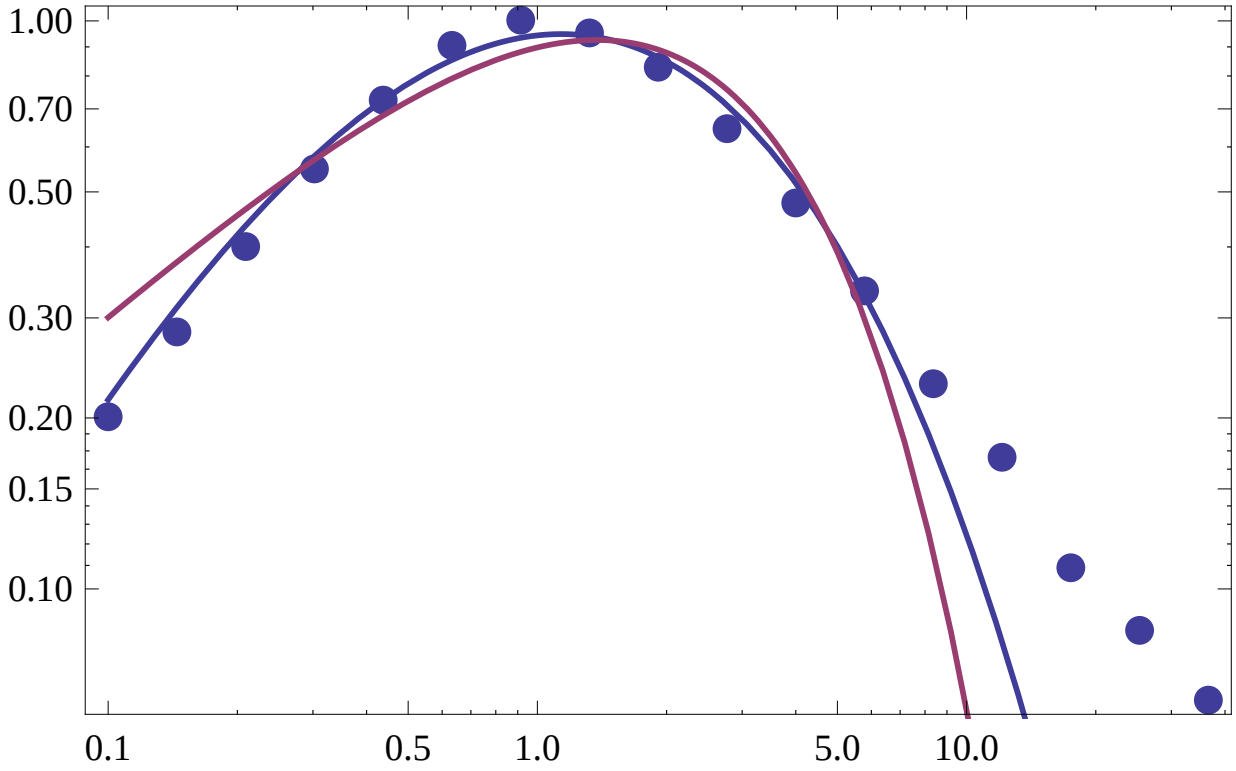

Fig. 10.— Numerical fit to the function $f = 2/(x + 1/x)$ using a softened exponential function, $\propto \epsilon^{\alpha} e^{-(\epsilon/\epsilon_{br})^{b}}$. Two curves correspond to extreme values of the parameters ($\epsilon_{br} = 0.01$, $\alpha = 1.87$, $b = 0.35$ and $\epsilon_{br} = 2$, $\alpha = 1.68$, $b = 0.98$), but both give acceptable fits (reduced $\chi^2 = 0.33$ and 1.01 correspondingly.)